Transformation of photoluminescence and Raman scattering spectra of Si-rich Al2O3 films at thermal annealing

ARTICLE *in* PHYSICA B CONDENSED MATTER · NOVEMBER 2014

Impact Factor: 1.32 · DOI: 10.1016/j.physb.2014.05.032

Tetyana V. Torchynska
Instituto Politécnico Nacional

Physica B 453 (2014) 107–110

Contents lists available at ScienceDirect

Physica B

journal homepage: www.elsevier.com/locate/physb

Transformation of photoluminescence and Raman scattering spectra of Si-rich Al_2O_3 films at thermal annealing

E. Vergara Hernandez [a], T.V. Torchynska [b,*], J. Jedrzejewski [c], I. Balberg [c]

[a] UPIITA-Instituto Politecnico Nacional, Mexico DF 07320, Mexico
[b] ESFM-Instituto Politecnico Nacional, Mexico DF 07320, Mexico
[c] Racah Institute of Physics, Hebrew University, 91904 Jerusalem, Israel

ARTICLE INFO

Available online 27 May 2014

Keywords:
Si-rich Al2O3 films
Photoluminescence
Raman scattering
Si nanocrystals

ABSTRACT

The effect of thermal annealing on optical properties of Al_2O_3 films with the different Si contents was investigated using the photoluminescence and Raman scattering methods. Si-rich Al_2O_3 films were prepared by RF magnetron co-sputtering of Si and Al_2O_3 targets on long quartz glass substrates. Photoluminescence (PL) spectra of as grown Si-rich Al_2O_3 films are characterized by four PL bands with the peak positions at 2.90, 2.70, 2.30 and 1.45 eV. The small intensity Raman peaks related to the scattering in the amorphous Si phase has been detected in as grown films as well.

Thermal annealing at 1150 °C for 90 min stimulates the formation of Si nanocrystals (NCs) in the film area with the Si content exceeded 50%. The Raman peak related to the scattering on optic phonons in Si NCs has been detected for this area. After thermal annealing the PL intensity of all mentioned PL bands decreases in the film area with smaller Si content ($\leq$50%) and increases in the film area with higher Si content ($\geq$50%). Simultaneously the new PL band with the peak position at 1.65 eV appears in the film area with higher Si content ($\geq$50%). The new PL band (1.65 eV) is attributed to the exciton recombination inside of small size Si NCs (2.5–2.7 nm). In bigger size Si NCs (3.5–5.0 nm) the PL band at 1.65 eV has been not detected due to the impact, apparently, of elastic strain appeared at the Si/Al_2O_3 interface.

Temperature dependences of PL spectra for the Si-rich Al_2O_3 films have been studied in the range of 10–300 K with the aim to reveal the mechanism of recombination transitions for the mentioned above PL bands 2.90, 2.70, 2.30 and 1.45 eV in as grown films. The thermal activation of PL intensity and permanent PL peak positions in the temperature range 10–300 K permit to assign these PL bands to defect related emission in Al_2O_3 matrix.

1. Introduction

Light emitting Si nanocrystals (NCs) in the SiO_2 matrix were studied intensively during the last 20 years due to their attractive perspectives for optoelectronics, microelectronics and photonics connected with the possibility to joint in a single chip the Si base devices for the realization of short scale optic interconnections [1–3]. Other promising application of Si NCs is expected in biology owing to the low Si toxicity in comparison with the II–VI semiconductor quantum dots widely used for the image production [4,5]. Si NCs in dielectric matrix are interesting as well for the charge trapped nonvolatile memory devices [6]. The different types of matrices (SiO_2, ZrO_2, HfO_2, Al_2O_3) have been studied for the application of Si NCs in nonvolatile memory devices [7,8]. The Al_2O_3 matrix is interesting from the point of view of the essential bound energy and the high radiation and chemical durability of this material [9]. Additionally the amorphous phase Al_2O_3 is characterized by high thermal conductivity, exceptional mechanical properties and a wide range of transparency [10]. In this paper the luminescence properties of Si-rich Al_2O_3 films obtained by RF magnetron spattering will be presented.

2. Experimental details

Si-rich Al_2O_3 films were deposited by radio frequency (RF) magnetron co-sputtering from two targets (Si and Al_2O_3) in an argon plasma on a long quartz glass substrate (type GE 124) a 10-mm width and a 140-mm length as it is shown in Fig. 1. Four groups of samples (2, 4, 8, 10), entitled as it is shown in Fig. 1, with the different contents of Si were chosen for the investigation in as grown state (A). Then the Si-rich Al_2O_3 films were annealed at 1150 °C for 90 min in

* Corresponding author.
E-mail addresses: ttorch@esfm.ipn.mx, ttorch85@yahoo.com.mx (T.V. Torchynska).

http://dx.doi.org/10.1016/j.physb.2014.05.032

ambient air to form the Si NCs inside of the Al_2O_3 matrix. Annealed samples are mentioned as 2B, 4B, 8B, 10B in the text. PL spectra were measured at the excitation by a He–Cd laser with a wavelength of 325 nm and a beam power of 80 mW at 10–300 K using a PL setup on a base of spectrometer SPEX500 described in Refs. [11,12]. The Si volume content (given in units of vol%) was estimated earlier as a function of the position along of the substrate and varied in the range of 15–20 vol% (Si poor side) up to 65 vol% (Si rich side) [13,14].

3. Experimental results and discussion

The Raman scattering spectra of as grown Si rich—Al_2O_3 films (not shown) are characterized by small intensity Raman peaks related, apparently, to the scattering in the amorphous Si phase. Thermal annealing at 1150 °C for 90 min stimulates the formation of Si nanocrystals (NCs) in the film area with the Si content exceeded 50% (Fig. 2). The Raman peak related to the light scattering by optic phonons in silicon NCs has been detected in the area with the Si content of 50–60 vol% (samples 2B and 4B). In the film area (8B, 10B) with the Si content (15–25 vol%) the wide small intensity Raman scattering band has been detected. This Raman band is the superposition of the Raman peaks related to the scattering by TA (~145 cm^{-1}), LA (~400 cm^{-1}) and TO/LO (482–485 cm^{-1}) phonons in the amorphous Si phase [1]. The position and width of Raman peaks and the estimated sizes of Si NCs [15,16] have been presented in Table 1 for the studied group of samples. The "red" shift of Raman peaks, related to the scattering on LO phonons in Si NCs (502–506 cm^{-1}), respectively of its position in the bulk Si crystals (520 cm^{-1}) permits to use the phonon confinement model for the estimation of Si NC sizes [15,16].

PL spectra of studied samples in as grown (A) and thermal annealed (B) states have been presented in Figs. 3 and 4, respectively. In the as grown state four overlapped PL bands with the peak positions at 2.90, 2.70, 2.30 and 1.45 eV clearly have been seen in PL spectra. It was shown early [14] that the Si concentration CSi in long range Si-rich Al_2O_3 or SiO_2 films varied from 15 vol% (10A) to 65 vol % (1A). Thus all PL bands in the as grown state are characterized by the highest PL intensities in the samples 8A, 10A with the minimum Si content (15–25%). With increasing the Si content in films the PL intensity of all PL bands decreases monotonically (Fig. 3).

Thermal annealing of the Si-rich Al_2O_3 films at 1150 °C for 90 min stimulates the formation of Si NCs [13,14]. After thermal annealing the PL intensity of mentioned above PL bands decreases in the film area with the smaller Si content (8B, 10B) and increases in the film area with higher Si content (2B, 4B) (Fig. 4). The last effect is related, apparently, to the transparency increasing the Si-rich Al_2O_3 films after the formation of Si NCs. Simultaneously the new PL band appears with the peak position at 1.65 eV in the film with the Si content around 60%. The new PL band (1.65 eV) is attributed to the exciton recombination inside of Si NCs [1]. It is essential to note that the Si NCs of different sizes (Table 1) were detected using Raman scattering in 2B and 4B samples, but the new PL band appears only in the sample 2B with the smallest Si

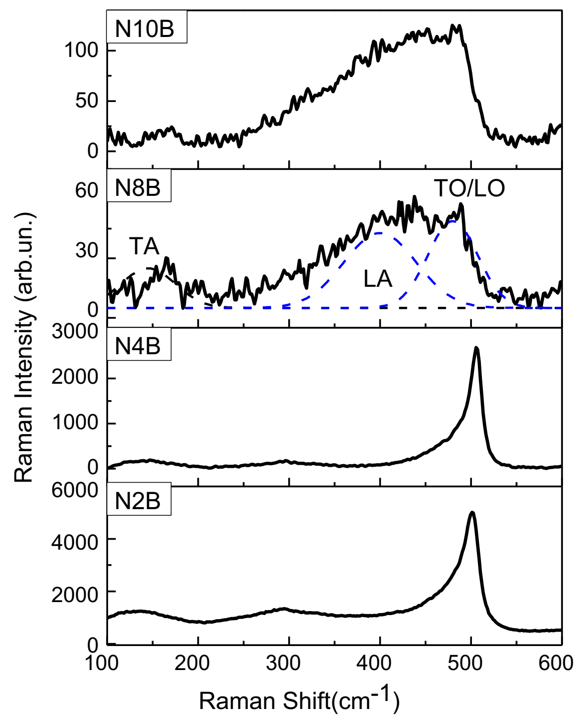

Fig. 2. Raman scattering spectra of annealed Si-rich Al_2O_3 samples measured at 300 K.

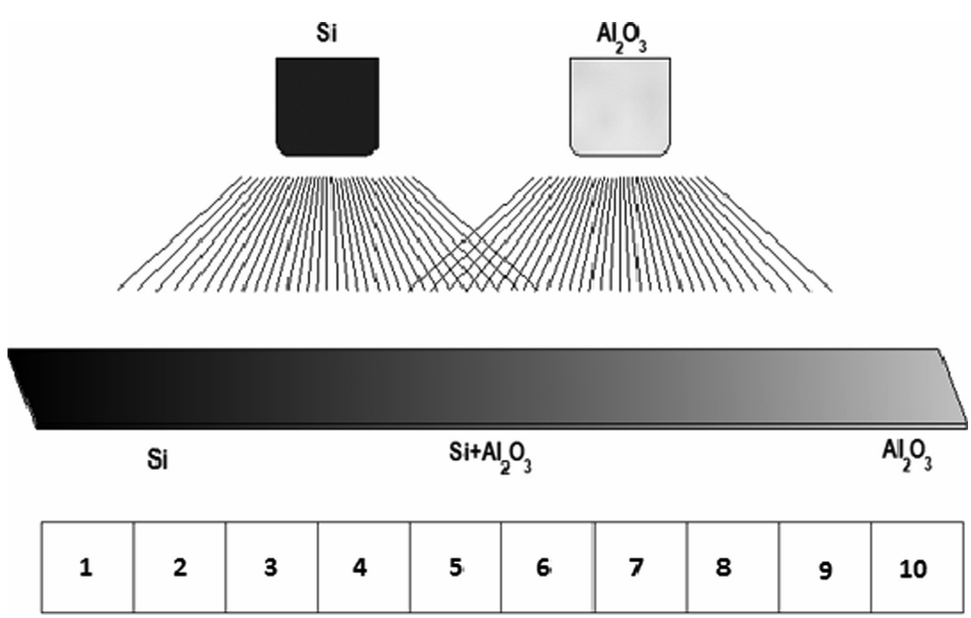

Fig. 1. The scheme of RF spattering of Si-rich Al_2O_3 films.

Table 1
Parameters of studied samples and Raman peaks.

Number	Si content (%)	TO/LO Raman peak (cm^{-1})	Width of Raman peak (cm^{-1})	Si NC size (nm) [15,16]
2B	60	502	25	2.5–2.7
4B	50	506	20	3.5–5.0
8B	25	487		
10B	15	482		

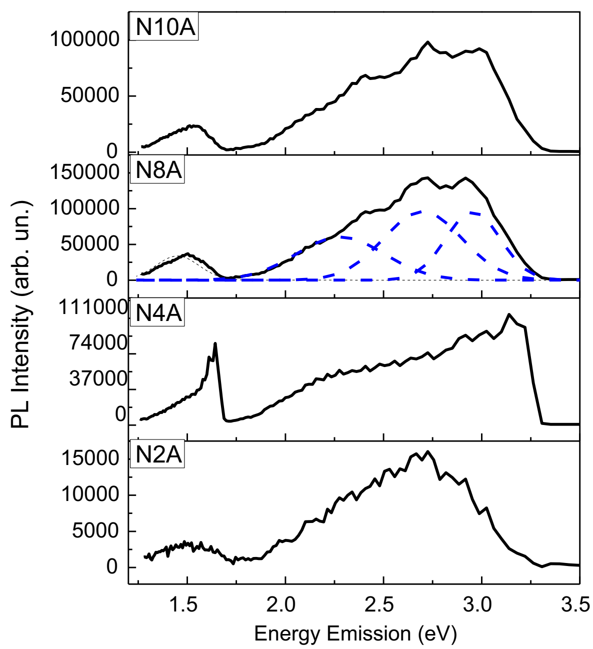

Fig. 3. PL spectra of freshly prepared Si-rich Al_2O_3 samples measured at 300 K.

NC size (2.5–2.7 nm). The last fact can be attributed (i) to the growth of the oscillation strength for the exciton recombination in smallest size Si NCs or (ii) to the negative impact of elastic strain appeared at the Si/Al_2O_3 interface in the bigger size (3.5–5.0 nm) Si NCs. Note, that the lack of PL signal from the Si nanocrystals was detected earlier and assigned to the large stress on Si nanocrystals in the Al_2O_3 matrix for as grown samples in Refs. [17,18]. It is essential that annealing in oxidizing atmosphere leads to the emission appearance of Si NCs due to the strain reduction when the SiO_2 shells formed around Si NCs [19]

The temperature dependences of PL spectra of Si-rich Al_2O_3 films have been studied in the range of 10–300 K with the aim to reveal the mechanism of recombination transitions for the PL bands centered at 2.90, 2.70, 2.30 and 1.45 eV (Fig. 5). The PL intensity of all PL bands increases monotonously versus temperature due to the activation of optical transitions as it is clear from Fig. 5. Permanent PL peak positions in the temperature range 10–300 K permit assigning these PL bands to the defect related emission in the Al_2O_3 matrix. Actually the orange emission (~2.06–2.18 eV) of Al_2O_3 films was investigated earlier and attributed to the F^{2+} centers in Al_2O_3 [20,21]. The blue defect related emission of Al_2O_3 films was reported as well [22,23]. The emission at 2.90 eV in Al_2O_3 has been ascribed to F centers [23]. The green emission (500 nm) in Al_2O_3 was earlier attributed to Al_i^+ ion [9,24]. The nature of 1.45 eV PL band is not clear. Actually the synchronous decreasing the PL intensities of 1.45 and 2.90 eV bands with the Si content rise permits to assign of the 1.45 eV PL band to the second order diffraction of 2.90 eV emission [25].

The annealing of Si-rich Al_2O_3 films in ambient air stimulates both the oxidation process in the Al_2O_3 matrix and the occupation

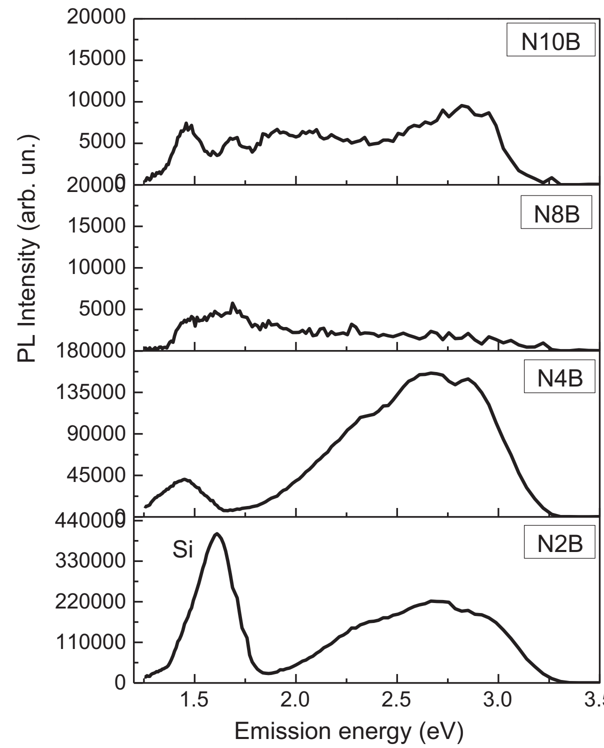

Fig. 4. PL spectra of annealed Si-rich Al_2O_3 samples measured at 300 K.

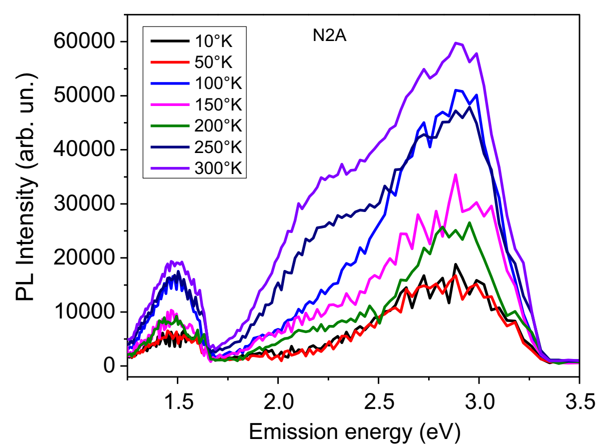

Fig. 5. PL spectra of the sample 8A measured at different temperatures of 10–300 K.

of Al vacancies by the Si atoms. These processes are accompanied by a reduction of defect concentrations in the Al_2O_3 matrix and, as a result, by decreasing the PL intensity of defect related PL bands (Fig. 4, 8B, 10B). Simultaneously, after the annealing the PL intensity increases in the film area with higher Si content (Fig. 4, 2B, 4B), apparently, owing to the transparency increasing the Si-rich Al_2O_3 films after the formation of Si NCs.

4. Conclusion

The effect of thermal annealing on photoluminescence of Al_2O_3 films with the different Si content was investigated. PL bands in as grown Si-rich Al_2O_3 films have been studied and assigned to defect related emission in the Al_2O_3 matrix. Thermal annealing of Si-rich Al_2O_3 films at 1150 °C for 90 min stimulates the formation of Si NCs with different sizes which depend on the Si content in the film. The new PL band with the peak at 1.65 eV related to the exciton emission in Si NCs appears in the PL spectrum of the sample with the Si content of 60%. Note, that in the sample with the big size Si NCs (3.5–5.0 nm) the PL band related to exciton emission in NCs has been not detected. The last fact is attributed to the negative impact of elastic strain at the Si/Al_2O_3 interface for the big size Si NCs embedded in the Al_2O_3 matrix.

Acknowledgments

The authors would like to thank the CONACYT (project 130387) and SIP-IPN, Mexico, for the financial support and the Dr. J.L. Casas Espinola for the PL measurement.

References

[1] T.V. Torchynska, Si and Ge Quantum Dot Structures, in Book: Nanocrystals and Quantum Dots of Group IV Semiconductors, in: T.V. Torchynska, Vorobiev Yu. (Eds.), American Scientific Publisher, Stevenson Ranch, CA, USA, 2010, pp. 42–84.
[2] M. Salib, M. Morse, L. Liao, Intel Technol. J. 8 (2) (2004).
[3] G.T. Reed, Nature 427 (6975) (2004) 595.
[4] X. Michalet, F.F. Pinaud, L.A. Bentolila, Science 307 (5709) (2005) 538.
[5] Z.F. Li, E. Ruckenstein, Nano Lett. 4 (8) (2004) 1463.
[6] Zs.J. Horváth, P. Basa, Nanocrystal Memory Structures in the Book: Nanocrystals and Quantum Dots of Group IV Semiconductors, in: T.V. Torchynska, Vorobiev Yu. (Eds.), American Scientific Publisher, Stevenson Ranch, CA, USA, 2010, pp. 225–252.
[7] E. Talbot, M. Roussel, C. Genevois, P. Pareige, L. Khomenkova, X. Portier, F. Gourbilleau, J. Appl. Phys. 111 (2012) 103519.
[8] L. Bi, J.Y. Feng, J. Lumin. 121 (2006) 95.
[9] N. Kristianpoller, A. Rehavi, A. Shmilevich, D. Weiss, R. Chen, Nucl. Instrum. Methods Phys. Res., Sect. B 141 (1998) 343.
[10] Xh. Xiao, R. Serna, C.N. Afonso, I. Vickridge, Appl. Phys. Lett. 87 (2005) 111103.
[11] T.V. Torchynska, Nanotechnology 20 (2009) 095401.
[12] T.V. Torchynska, A. Diaz Cano, M Dybic, S. Ostapenko, M Mynbaeva, Physica B 376–377 (2006) 367.
[13] N. Korsunska, T. Stara, V. Strelchuk, O. Kolomys, V. Kladko, A. Kuchuk, L. Khomenkova, J. Jedrzejewski, I. Balberg, Physica E 51 (2013) 115.
[14] I. Balberg, Physica E 51 (2013) 2.
[15] Zh. Sui, P.P. Leong, I.P. Herman, G.S. Higashi, H. Temkin, Appl. Phys. Lett. 60 (1992) 2086.
[16] Md. N. Islam, S. Kumar, Appl. Phys. Lett. 78 (2001) 715.
[17] S. Yerci, U. Serincan, I. Dogan, S. Tokay, M. Genisel., A. Aydinli, R. Turan, J. Appl. Phys. 100 (2006) 074301.
[18] D.I. Tetelbaum, A.N. Mikhaylov, A.I. Belov, A.V. Ershov, E.A. Pitirimova, S. M. Plankina, V.N. Smirnov, A.I. Kovalev, R. Turan, S. Yerci, T.G. Finstad, S. Foss, Phys. Solid State 51 (2009) 409.
[19] A.N. Mikhaylov, A.I. Belov, A.B. Kostyuk, I. Yu., D.S. Zhavoronkov, A.V. Korolev, A.V. Nezhdanov, D.V. Ershov, T.A. Guseinov, N.D. Gracheva, E.S. Malygin, D. I. Demidov, Phys. Solid State 54 (2012) 368.
[20] S. Yin, E. Xie, C. Zhang, Z. Wang, L. Zhou, I.Z. Ma, C.F. Yao, H. Zang, C.B. Liu, Y. B. Sheng, J. Gou, Nucl. Instrum. Methods B 12–13 (2008) 2998.
[21] I. Dogan, I. Yildiz, R. Turan, Physica E 41 (2009) 976.
[22] Y.-T. Chen, Ch.-L. Cheng, Y.-F. Chen, Nanotechnology 19 (44) (2008) 5707.
[23] K.H. Lee, J.H. Crawford Jr., Phys. Rev. B: Condens. Matter 15 (1977) 4065.
[24] M.S. Akselrod, V.S. Kortov, Radiat. Prot. Dosim. 33 (1990) 123.
[25] C.-A. Lin, D.-S. Tsai, C.-Y. Chen, J.-H. He, Nanoscale 3 (2011) 1195.